Journal of Archaeological Science: Reports 61 (2025) 104894

Contents lists available at ScienceDirect

Journal of Archaeological Science: Reports

journal homepage: www.elsevier.com/locate/jasrep

Preservation of $\delta^{13}C$ signatures in oak charred wood: Application to the "forest" of Notre-Dame de Paris

Eva Rocha [a,*], Alexa Dufraisse [b], Katja T. Rinne-Garmston [c], Elina Sahlstedt [c], Mercedes Mendez-Millan [d], Thanh Thuy Nguyen Tu [e], Olivier Girardclos [f], Michel Lemoine [b], Amir Ghavidel [g], Lucas Terrei [h], Anthony Collin [h], Ludovic Bellot-Gurlet [i], Frédéric Delarue [e]

[a] UMR 7209 - AASPE-MNHN, Archéozoologie, Archéobotanique: Sociétés, Pratiques et Environnements, CP56, 55 rue Buffon, 75005, Paris, France
[b] UMR 7209 – AASPE-CNRS/MNHN, Archéozoologie, Archéobotanique: Sociétés, Pratiques et Environnements, CP56, 55 rue Buffon, 75005 Paris, France
[c] Natural Resources Institute Finland (Luke), Latokartanonkaari 9, 00790 Helsinki, Finland
[d] IRD, SU, CNRS, MNHN, IPSL, LOCEAN : Laboratoire d'Océanographie et du Climat: Expérimentations et Approches Numériques, Bondy, France
[e] CNRS, EPHE, PSL, UMR 7619 METIS, Sorbonne Université, 4 place Jussieu, 75005 Paris Cedex 05, France
[f] UMR 6249 Chronoenvironnement CNRS, Université de Franche-Comté, Besançon, France
[g] School of Engineering, University of Northern British Columbia, 499 George St., Prince George V2L1R7, British Columbia, Canada
[h] Université de Lorraine, CNRS, UMR 7563 LEMTA, Nancy, France
[i] Sorbonne Université, CNRS, de la Molécule aux Nano-objets: Réactivité, Interactions et Spectroscopies, MONARIS, 4 Place Jussieu, 75005 Paris, France

ARTICLE INFO

Keywords:
Carbon isotope
Inter- and intra-annual signal
Deciduous oak
Laser ablation
Charcoal
Wood

ABSTRACT

The fire of the Notre-Dame de Paris's cathedral (NDP) in 2019 brought a unique opportunity to study the past environmental conditions in the region during the High Middle Ages through the charred oak beams of the "Forest" (name given to its framework). However, as a preamble, there is a need to evaluate the preservation of the stable carbon isotope signatures ($\delta^{13}C$) in response to changes in molecular composition, occurring with carbonisation. To this end, experimental studies were conducted on modern and NDP oak wood at both inter- and intra-annual levels. Laser ablation was used for the first time on burnt wood. Results show that regardless of the charring duration, at temperatures above 500 °C, carbonisation-induced ^{13}C fractionation shows a consistent decrease ($\Delta^{13}C$) of approximately 1 ‰ relative to uncharred values. Despite a slight decrease in variance, a strong and significant correlation ($r_{mean} = 0.9$, $p < 0.01$) was observed between the uncharred time series and the carbonised counterpart, showing that the C isotopic variability is preserved. This study paves the way to use the charcoal remains from the Notre-Dame de Paris framework as a unique paleoenvironmental archive.

1. Introduction

Nicknamed "the forest" because of the hundreds of timbers used in its construction, the oak frame of the Notre-Dame de Paris's cathedral (NDP) is one of the greatest masterpieces of Gothic carpentry in France (Hoffsummer, 2009). It is estimated that between 800 and 1,000 oak trees were used in its construction, with each large beam coming from a different tree. Felled between the 12th and 13th centuries, the wooden frame provides a unique window into the Middle Ages oak forest surrounding the Paris Bassin (Štulc, 2023). Following the fire of April 2019, the remaining beams exhibited various degrees of carbonisation (Fig. 1). Some pieces were only partially burnt, while others were charred to the wood core, with carbonisation temperatures estimated between 500 °C and 1300 °C (Deldicque and Rouzaud, 2020).

Tree-ring studies, namely those focusing on the $\delta^{13}C$ signatures, have become a standard application in palaeoenvironmental assessments to document and verify a myriad of environmental changes (Siegwolf et al., 2022). $\delta^{13}C$ in wood mainly reflects the balance between stomatal conductance and photosynthetic rate and the influence of their environmental drivers, such as soil water content, trees' evaporative demand, site fertility, and light availability (McCarroll and Loader, 2004; Siegwolf et al., 2022). Consequently, $\delta^{13}C$ in tree rings has been widely used to assess past environmental conditions, e.g. CO_2 concentrations (Zhao et al., 2006), air temperature (Esper et al., 2015; Young et al., 2012), precipitation (Leavitt et al., 2007; Liu et al., 2008) and sunshine variability (Hafner et al., 2014; Loader et al., 2013). While well

* Corresponding author.
E-mail address: eva.rocha@mnhn.fr (E. Rocha).

https://doi.org/10.1016/j.jasrep.2024.104894
Received 10 May 2024; Received in revised form 8 November 2024; Accepted 20 November 2024
Available online 1 December 2024

Fig. 1. Example of the carbonisation heterogeneity in the wood beams recovered from the Notre-Dame de Paris cathedral.

established as a proxy for paleoenvironmental reconstructions based on living trees or relict wood stems (Edvardsson et al., 2014; Esper et al., 2018; Helama et al., 2018; Masson-Delmotte et al., 2005), $\delta^{13}C$ has also become an important tool in the investigation of wood charcoals from archaeological settings (Aguilera et al., 2009; Caracuta et al., 2016; Dufraisse et al., 2022; Fiorentino et al., 2015). Occurring as a testimony of anthropic activities (including domestic firewood or fuel waste from kilns), archaeological charcoals result from wood carbonisation in the absence of oxygen (Braadbaart and Poole, 2008; Scott, 2010). As a consequence of the preferential thermal degradation of the ^{13}C-enriched cellulose and hemicellulose, carbonisation yields a progressive decrease in $\delta^{13}C$ tightly related to heating temperature (Ascough et al., 2008; Audiard et al., 2018; Czimczik et al., 2002; Mouraux et al., 2022). Following the relationship between heating temperature and ^{13}C fractionation, the wood's original $\delta^{13}C$ has been estimated and used as a proxy to assess past climate and environmental variability (Aguilera et al., 2012; Ferrio et al., 2006; Hall et al., 2008). Although promising, this approach is still incomplete as it has not been straightforwardly demonstrated that $\delta^{13}C$ variations are preserved against carbonisation. Additionally, many studies on ^{13}C fractionation during charcoalification have analysed charcoal as a whole without distinguishing between individual growth rings. This approach may not fully capture the $\delta^{13}C$ variability among different wood components (e.g., heartwood vs. sapwood or earlywood vs. latewood)(Borella et al., 1998).

Annually-resolved time series of $\delta^{13}C$ not only serve as a record of past climate and environmental changes but also offer valuable insights into trees' response to such variations, especially in years where distinct radial growth reactions occur (e.g. narrow rings). Isotopic signatures can also provide detailed information at the sub-annual resolution (i.e., earlywood (EW) and latewood (LW)), revealing changes within the growing season that might help distinguish exogenous factors, such as forest management practices (competition control and thinning treatments), from the direct effects of climate variability (e.g. cold/wet or warm/drought periods) (Marshall et al., 2022). Additionally, EW and LW features, formed during spring and summer, respectively, record distinct climatic signals that could be masked by inter-annual variability when analysing the whole ring (Rinne et al., 2015). However, such an intra-annual approach is rarely applied to the study of ancient charcoals (Baton et al., 2017) due to technical limitations related to the physical state of friability and shrinkage of samples (Blondel et al., 2018; Paradis-Grenouillet and Dufraisse, 2018). Recent technological advances in analytical techniques, notably the use of laser ablation coupled to IRMS, can overcome this methodological issue, providing the possibility to retrieve environmental information from tree-ring parameters, currently overlooked in dendro-anthracology (review in Dufraisse et al., 2022).

In this study, we aim to assess the preservation of $\delta^{13}C$ in oak wood after carbonisation. To this end, we investigated inter- and intra-annual $\delta^{13}C$ variability in (i) experimentally charred modern deciduous oak wood and (ii) charred oak wood from Notre-Dame de Paris. Following this, we further discuss the feasibility of using charred wood from Notre-Dame roof frame as a unique environmental archive to assess paleoenvironmental conditions prevailing in the Paris Basin between the 11th and 13th centuries.

2. Material and methods

2.1. Reference – archaeological tree-ring data and experimental carbonisation

Samples were collected from a 1.5 m length sessile oak (*Quercus petraea* Liebl.) tree stem (Fig. 2a) growing in the Fontainebleau forest (northern France; 48°25′N, 2°37′E), an area that has been providing the source material for several dendroclimatological studies (Etien et al., 2008; Labuhn et al., 2016). A total of 5 cubes ($\approx 5 \times 5$ cm^2) were cut from the heartwood (including the pith). The cubes were kept in an oven at a temperature of 20 °C for several weeks. Before carbonisation, one thin disc was cut from each cube and used as a reference. The annual ring widths (RW) of each disc were measured and crossdated using a sliding measuring table connected to the Time Series Analysis Programme (TSAP-Win) software (Rinntech, Heidelberg, Germany) and the COFECHA program used to verify the accuracy of the measurements (Grissino-Mayer, 2001). The series was dated to 1914–2021 CE (Fig. 3a). Using a cone calorimeter from Fire Testing Technology (FTT) (Terrei et al., 2019, Fig. 2b), each cube was individually subjected to a heat flux of 80 kw/m^2 for durations of 12, 20, 24, 28 and 32 min. This exposure leads to surface temperatures reaching up to 900 °C. An infrared camera (ORION SC7000 by Flir with a specific optic filter at 2564 cm-1) was used to measure the surface temperature of each cube. At the same time, 12 Type-K thermocouple sensors (Ø 0.1 mm) were placed at varying distances from the charred front in an additional cube designated for control purposes. Precisely, ten thin wire thermocouples were positioned every 2 mm, from 2 to 20 mm depth, and two more at 30 and 40 mm (Fig. 2c) according to the procedures described in Terrei et al. (2021). The distance between the cone and the samples was set to 25 mm to obtain a homogeneous heat flux over the entire exposed surface. Immediately after exposure, the samples were immersed in liquid nitrogen to stop the carbonisation process. To avoid fragmentation, the samples were protected with thermo-retractable bands (i.e., a plastic tube that shrinks when heated) following the procedure described in Brossier and Poirier (2018).

For the archaeological sample, a 24-year sequence of rings from a beam recovered from the roof structure of NDP, presenting both charred and uncharred sections, was used in this study for comparative purposes with the modern carbonisation experiment (Fig. 2d). The sample was dated by dendrochronology to 1133–1177 CE (Penagos et al., 2022) (Fig. 3b).

2.2. Inter- and intra-annual stable carbon isotope sampling, measurements, and analysis

After carbonisation, the cubes were cut into smaller discs using a diamond wire saw. Both reference (i.e. uncharred) and charred wood were sampled in equivalent sections. Annual whole rings from 1919 to 1933 were separated using a drill (Ø 0.5–0.8 mm) under a binocular. Two radii were sampled to account for circumferential variability (Leavitt, 2010), and approximately 1.5–2 mg of fine homogeneous powder was obtained per calendar year.

The NDP sample was prepared using the same procedure as the experimental wood. Due to the different degrees of carbonisation in the NDP sample, the two-radii strategy was not always possible, particularly

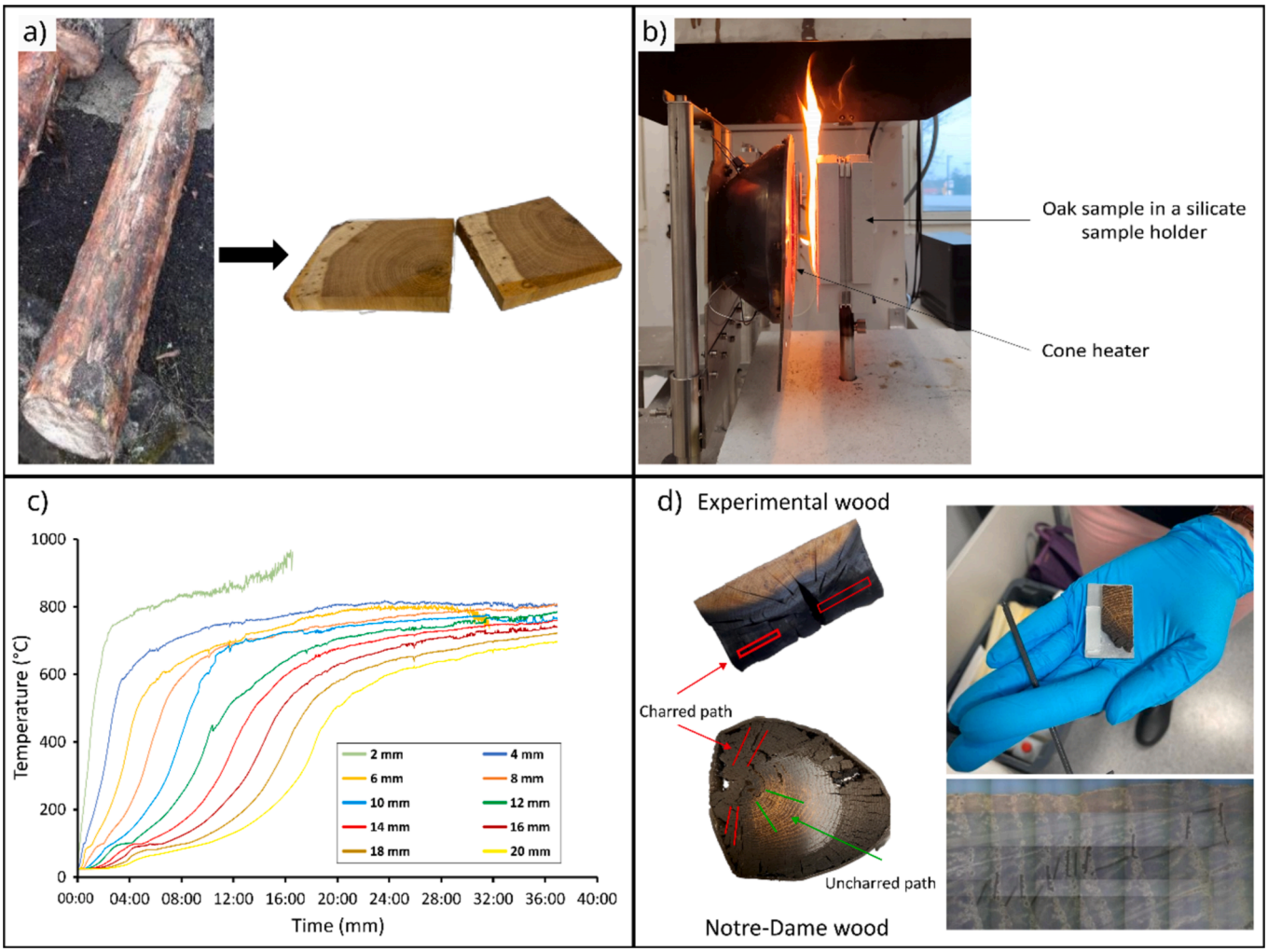

Fig. 2. Overview of some of the materials and methods used in this study. (a) Oak tree stem and sampled cubes. (b) Cone heater setup. (c) Examples of the temperature evolution recorded by the thermocouples during the carbonisation experiment. (d) Experimental and Notre-Dame wood samples (with charred and uncharred paths marked) and an example of the wood lath measured by the laser ablation method (LA-IRMS).

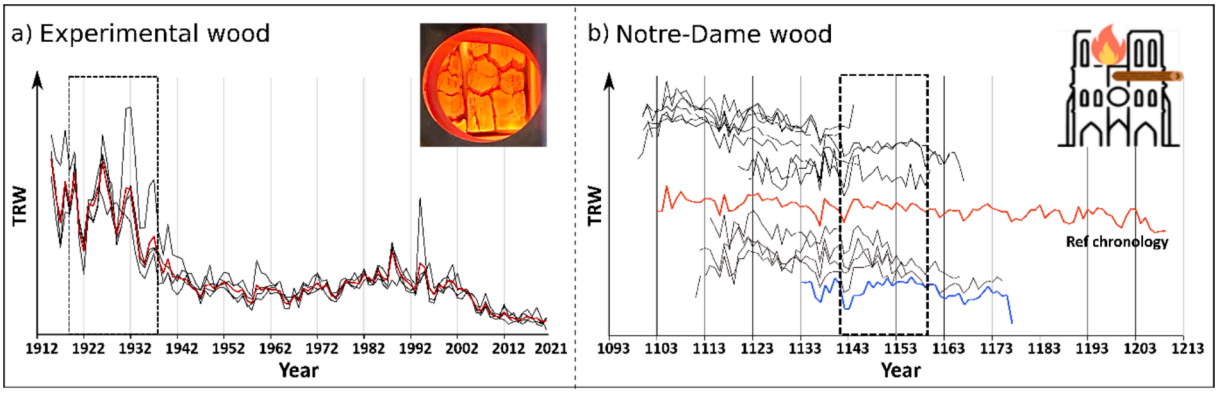

Fig. 3. (a) Tree ring width (TRW) data from the five samples used in this study and their mean chronology (red). (b) TRW data from NDP carbonised samples. The red line represents the mean chronology used for dendrochronological dating, and the blue line is the sample used in this study for the $\delta^{13}C$ analysis. The dashed areas indicate the period in analysis for both samples (i.e., 1919–1935 for the experimental wood and 1135–1158 for the NDP).

for the uncarbonised portion (see Fig. 2d). In such cases, a larger circumferential path within the respective charred and uncharred sections of the sample (avoiding the intermediate zone) was preferred to obtain a similar mass as for the experimental wood samples. Powdered subsamples (0.15–0.2 mg) were then packed in tin foil capsules and combusted using an elemental analyser Flash HT 2000 coupled to an Isotope Ratio Mass Spectrometer Delta V advantage (EA-IRMS) from Thermo Fisher Scientific to determine the 13C/12C ratio. The analysis was performed at the ALYSES facility, located at the Institut de Recherche pour le Développement (IRD-SU), France. The spectrometer

was calibrated against VPDB using two certified reference materials, the IAEA-CH3 (Cellulose) and the EMAP2. Uncharred oak standard was used as an internal control to assess the reproducibility and accuracy of $\delta^{13}C$ measurements (Baton et al., 2017; Mouraux et al., 2022) and indicates an analytical uncertainty of ± 0.1 ‰ on $\delta^{13}C$ values.

The intra-annual analysis of $\delta^{13}C$ values was performed through laser ablation isotope ratio mass spectrometry (LA-IRMS) (Teledyne Photon Machines LSX-213 G2+, and Sercon 2022 RMS) at Stable Isotope Laboratory of Luke (SILL), located at the Natural Resources Institute Finland (Luke). Periods of 6 and 8 years (1919–1924 and 1139–1146) were identified for the experimental and NDP wood, respectively. The above periods were selected to include the extremely narrow rings of 1921–1922 (≈1.2 mm) for the experimental wood and 1142–1143 (≈1.0 mm) for the NDP. The samples were analysed twice per growth ring for both earlywood (EW) and latewood (LW) isotopic composition. A laser beam of 100 μm in diameter was used at a scan speed of 20 μm/s and a sampling length of 700 to 1800 μm. Two materials, USGS-55 reference (Mexican ziricote wood, $\delta^{13}C = -27.13$ ‰) and an in-house reference material (yucca plant, $\delta^{13}C = -15.46$ ‰), were used for $\delta^{13}C$ data normalisation. Repeat measurements of a quality control material (IAEA-C3 cellulose paper) were analysed concurrently with the sample materials, indicating an uncertainty of < 0.2 ‰. The results for both methods were reported using the delta notation (δ) in parts per mil (‰) relative to the VPDB standard (Coplen, 1995).

2.3. Raman spectroscopy analysis

Raman spectroscopy analysis was used to determine the degree of aromaticity/condensation of the charcoals' chemical structure and to assess heating temperatures at the scale of individual growth rings. The analysis was performed on the 24-year carbonised sequence from NDP and compared to the experimental charcoal formed for 12 and 32 min, representing the lowest and highest carbonisation times of the experimental setup. While the experimental charcoal was immediately preserved with thermo-retractable bands, fragmentation during the various stages of storage and preparation of NDP samples resulted in the loss of the more brittle material from the outermost parts, where the highest thermal values are likely to be registered.

The Raman spectra were obtained with an HR800 Horiba Jobin Yvon spectrometer equipped with a 514 nm Ar + green laser and an ultra-narrow band BragGrate notch filter for Rayleigh filtering. A small amount of powder (few μg) from each ring was placed on a glass slide, and the laser beam focused on the sample with a long working distance of 50X objective. The laser power at the sample was set below one mW to prevent any thermal alteration of the charcoal during analysis (Everall, 1991). Raman spectra were then acquired after a time exposure of 40 s, repeated three times. For each sample, the Raman shift intensity was determined in the 600 to 2300 cm^{-1} spectral window (using a 600 line/mm grating), including the defect (D) and graphite (G) bands centred at about 1350 and 1600 cm^{-1}, respectively (Fig. 4a). After linear baseline corrections, the ratio between the height of the D and G bands (namely, the H_D/H_G ratio) was computed and used to assess the heating temperatures following the calibration curve provided in Deldicque et al. (2016) and Rouzaud et al. (2015). It is mainly the steady increase in the D-band height with increased temperatures, noticeable once carbonisation temperatures exceed 400 °C, that enables the estimation of the maximum temperatures at which a charcoal was formed. For a detailed characterisation of the evolution of the HD/HG ratios with temperature, see Deldicque et al., 2016, Deldicque and Rouzaud, 2020 and Mouraux et al., 2022.

2.4. Data analysis

Spearman's rank correlations were computed to assess the relationship between the uncharred and charred $\delta^{13}C$ time series. Observed isotope offsets, expressed as $\Delta^{13}C$, were calculated as the difference between the $\delta^{13}C$ determined on charred and uncharred samples ($\Delta^{13}C$ (‰) = $\delta^{13}C_{char} - \delta^{13}C_{unch}$). First-differenced (FD = Y_t-Y_{t-1}) data was used to assess the preservation of the year-to-year variability following carbonisation. The ANOVA test was applied to assess the differences in the carbonisation levels between the rings from the 12 and 32-minutes samples and those from the NDP sample.

3. Results

3.1. Raman spectroscopy

The Raman spectra obtained for the experimental charcoal samples at 12 and 32 min, as well as for NDP charcoal, showed statistically similar H_D/H_G ratios ($p = 0.1$) (Fig. 4b), with mean values of 0.61 ±

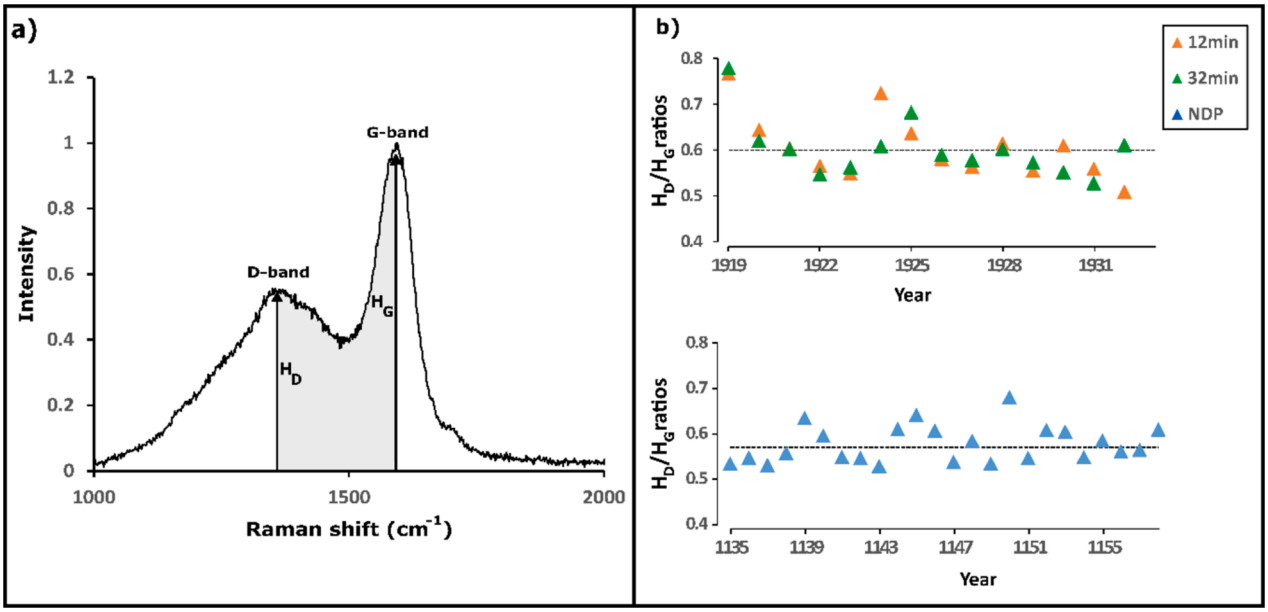

Fig. 4. (a) Raman spectrum of a charcoal sample from the experimental wood after normalisation with the D-band and G-band position. (b) H_D/H_G ratios determined by Raman spectroscopy in the annual rings of the NDP sample and experimental wood carbonised for 12 and 32 min.

0.07 (12 min), 0.60 ± 0.06 (32 min) and 0.57 ± 0.05 (NDP). Based on the calibration curve obtained from oak wood with a residence time of 1 h, as provided by Deldicque and Rouzaud (2020), these H_D/H_G ratios correspond to heating temperatures of ca. 600 — 700 °C.

Regarding the experimental charcoal, as shown in Fig. 4b, carbonisation time (12 or 32 min) has a negligible impact on the H_D/H_G ratio, with the measurements almost superimposed along the sampled transect. In both samples, the highest H_D/H_G ratios (0.77 and 0.78 for 12 and 32 min, respectively) are retrieved from the rings closest to the charred front and correspond to heating temperatures of ca. 750–800 °C (Deldicque and Rouzaud, 2020), in agreement with those determined by infrared camera and thermocouples (Fig. 2b). After these first rings, no clear carbonisation trend was observed in the measurements, with the H_D/H_G ratios fluctuating between 0.51 and 0.72. Similarly, the NDP sample displays a range of H_D/H_G ratios from 0.50 to 0.68, corresponding to heating temperatures between ca. 500 and 750 °C (Deldicque and Rouzaud, 2020).

3.2. Inter- and intra-annual $\delta^{13}C$ values

The $\delta^{13}C$ values measured at the inter-annual scale on the whole ring from the five reference samples (i.e., uncharred) ranged from −26.3 ‰ to –23.7 ‰ (mean $\delta^{13}C_{unch}$ = -25.1 ‰ ± 0.6) (Table 1). After carbonisation, the mean $\Delta^{13}C$ of all series was − 1.0 ‰ ± 0.3, with $\delta^{13}C_{char}$ values ranging from −26.8 ‰ to −24.6 ‰ (mean $\delta^{13}C_{char}$ = -26.0 ‰ ± 0.5). Despite the carbonisation-induced decrease in $\delta^{13}C$, strong and significant correlations ($r > 0.7$, $p < 0.01$) were observed between $\delta^{13}C$ values determined on the uncharred time series and their carbonised counterparts. Since carbonisation time had a negligible effect on the $\Delta^{13}C$, the five individual series were averaged to obtain a mean series for uncharred and charred data, and a correlation of 0.9, $p < 0.01$, was observed between the two series (Fig. 5a). First-differenced $\delta^{13}C$ data on the averaged series showed a coherent year-to-year variability (Fig. 6a) with the $\delta^{13}C$ values ranging from −1.1 ‰ to a maximum of 1 ‰ for the uncharred series and from −0.8 ‰ to a maximum of 0.8 ‰ for the charred samples.

For the NDP sample, uncharred $\delta^{13}C$ values varied from −25.6 ‰ to −23.4 ‰ (mean $\delta^{13}C_{unch}$ = −24.3 ‰ ± 0.5), whereas in carbonised rings, they ranged from −25.8 ‰ to −24.1 ‰ (mean $\delta^{13}C_{char}$ = −25.3 ‰ ± 0.4). In line with the findings for the experimental charcoal, the mean decrease in $\delta^{13}C$ was 0.9 ‰ ± 0.4 (Table 1). The correlation between the uncharred and charred time series was slightly lower than that observed for the experimental charcoals but remained highly significant ($r = 0.7$, $p < 0.01$) (Fig. 5b). In addition, the inter-annual $\delta^{13}C$ variability remained coherent, with $\delta^{13}C$ values ranging from −0.8 ‰ to a maximum of 1 ‰ for the uncharred series and from −0.7 ‰ to 0.6 ‰ for the charred series (Fig. 6b).

At the intra-annual scale, the laser ablation data of $\Delta^{13}C$ closely corresponded to the inter-annual variations observed at the whole ring level for both experimental and NDP samples. In experimental wood, the year-to-year early- and latewood variation ranged from −1.3 to 1.2 ‰ for uncharred samples and from −1 to 1.1 ‰ for charred samples (Fig. 7a), suggesting a high degree of signal preservation. For the NDP, EW exhibited a uniform pattern year-over-year, with minimal and preserved $\delta^{13}C$ variations ranging from −0.4 to 0.5 ‰ for both uncharred and charred samples. In contrast, for LW, the year-to-year $\delta^{13}C$ fluctuation was reduced, ranging from −0.7 to 1.1 ‰ before carbonisation to −0.3 to 0.6 ‰ following carbonisation (Fig. 7b).

4. Discussion and Conclusions

Carbonisation deeply modifies the physical, chemical, and structural properties of wood through mass loss, volume shrinkage, increased aromaticity and ^{13}C depletion (Bird and Ascough, 2012; Li et al., 2022). At the scale of a single plant species, the extent of these modifications depends mainly on the state of the wood (e.g., altered, damp, treated) and the carbonisation intensity (i.e. charring temperature and exposure time); therefore, assessing maximum charcoal formation temperatures is of utmost importance for the use of $\delta^{13}C$ as a paleoenvironmental proxy (Mouraux et al., 2022; Turney et al., 2006).

The paleothermometry method used in this study shows that both experimental and NDP charcoal samples exhibit heating temperature above 500 °C, a temperature threshold beyond which carbonisation has a limited effect on the $\delta^{13}C$ signatures (Fiorentino et al., 2015; Mouraux et al., 2022; Turney et al., 2006). The similar distribution of the H_D/H_G ratios observed among the three samples (Fig. 4b) indicates that the experimental charcoal underwent carbonisation intensities comparable to that of the NDP fire, at least for the more well-preserved wood remains that survived the heavy fragmentation processes. This consistency, therefore, enables the comparison between samples regarding the preservation of the $\delta^{13}C$ signatures. The generally higher H_D/H_G ratios measured in the first rings of the experimental charcoal are rather indicative of a more homogeneous carbonisation setup in terms of heat flow and exposed surface, with the progression of the combustion front from the core towards the outer layers of the beam. In the NDP samples, extreme thermal conditions are expected at the outermost part of the charcoal piece, due to the inverse carbonisation pattern, with the combustion front moving from the outer layers towards the core of the beam (Fig. 2d). The constant loss of material from the outermost parts of the NDP samples may have led to an underrepresentation of the most extreme thermal values, resulting in slightly lower HD/HG ratios.

The assessment on the preservation of the $\delta^{13}C$ signatures shows that charring duration had minimal impact on the $\Delta^{13}C$, as the values observed after 12 min of heating are identical to those after 32 min (Table 1). These results align with the findings of Turney et al. (2006), yet their observations were made after 30 min of heating. Previous work presented by Mouraux et al. (2022) on oak wood showed that significant $\delta^{13}C$ changes due to carbonisation primarily occur at temperatures below 400 °C, consistent with the early degradation of cellulose and hemicellulose, which are relatively enriched in ^{13}C (Ascough et al., 2008; Czimczik et al., 2002). This suggests that cellulose and hemicellulose were already degraded after 12 min of charring, thereby limiting the effect of a further increase in residence time on $\delta^{13}C$ signatures.

Overall, the average $\Delta^{13}C$ obtained in our study for both experimental and NDP charcoals was approximately 1 ‰, with a range from 0.1 to 1.6 ‰ (Table 1). This finding contrasts with the constant $\Delta^{13}C$ of

Table 1
Summary of the $\delta^{13}C$ (‰) and Raman spectroscopy data.

Carbonisation time	Mean $\delta^{13}C_{(unch)}$ (‰) ± SD	Range $\delta^{13}C_{(unch)}$ (min; max)	Mean $\delta^{13}C_{(charred)}$ (‰) ± SD	Range $\delta^{13}C_{(charred)}$ (min; max)	Mean $\Delta\delta^{13}C$* (‰) ± SD	Mean H_D/H_G ± SD	Range H_D/H_G (min; max)
12 min	−24.9 ± 0.6	(−25.7; −23.7)	−25.8 ± 0.5	(−26.7; −24.8)	−0.9 ± 0.3	0.61 ± 0.07	(0.51; 0.77)
20 min	−25.0 ± 0.6	(−25.8; −23.7)	−26.0 ± 0.5	(−26.8; −25.1)	−1.0 ± 0.3	n.d. **	n.d. **
24 min	−25.2 ± 0.6	(−26.2; −24.0)	−25.8 ± 0.6	(−26.8; −24.6)	−0.7 ± 0.2	n.d. **	n.d. **
28 min	−25.4 ± 0.6	(−26.3; −24.3)	−26.2 ± 0.5	(−26.8; −25.2)	−0.7 ± 0.4	n.d. **	n.d. **
32 min	−25.0 ± 0.5	(−25.9; −24.0)	−26.1 ± 0.4	(−26.5; −25.3)	−1.0 ± 0.3	0.60 ± 0.06	(0.53; 0.78)
Experimental (averaged series)	−25.1 ± 0.5	(−25.9; −24.0)	−26.0 ± 0.5	(−26.6; −25.1)	−0.9 ± 0.1	n.d. **	n.d. **
NDP	−24.3 ± 0.5	(−25.6; −23.4)	−25.3 ± 0.4	(−25.8; −24.1)	−0.9 ± 0.4	0.57 ± 0.04	(0.50; 0.68)

* $\Delta\delta^{13}C$ = difference between charred and uncharred values; ** n.d.: not determined.

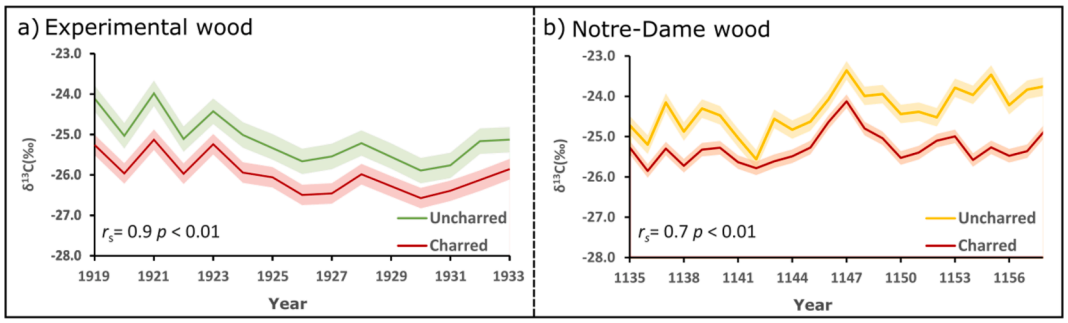

Fig. 5. Comparison between mean uncharred and mean charred time series for the (a) experimental wood (mean series obtained by averaging the five-individual series of uncharred and charred data) and (b) NDP sample. Shading areas indicate the 95% confidence interval.

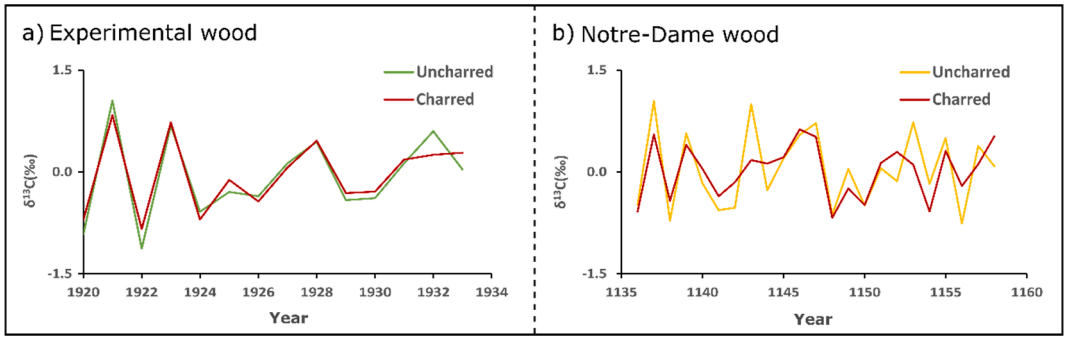

Fig. 6. $\delta^{13}C$ variability at the inter-annual scale (first-differenced values) for (a) the experimental (mean series obtained by averaging the five individual series of uncharred and charred data) and (b) NDP samples developed using the conventional bulk analysis (EA-IRMS).

1.8 ‰ and 1.4 ‰ reported by Mouraux et al. (2022) for *Quercus petraea* and Turney et al. (2006) for *Quercus robur*, respectively. Such contrast suggests that laboratory-produced charcoal experiments are not fully representative of the natural $\delta^{13}C$ variability of the wood. This is mainly due to the use of powdered samples and homogenisation techniques, and therefore, general corrections to estimate the wood's original $\delta^{13}C$ values should be applied with caution. In the context of the Notre-Dame project, measurement accuracy can be enhanced by increasing the number of radiis and trees analysed per year, as shown by averaging the series from the modern wood experiment (Fig. 5a).

Comparison of the first-differenced data (Fig. 6) showed a slight decrease in the inter-annual $\delta^{13}C$ variability between the uncharred and charred profiles for both experimental and NDP samples. The decrease is likely attributable to the different isotopic compositions of the wood constituents. Loader et al. (2003) showed that cellulose and lignin have different carbon isotope compositions, with lignin showing a slightly lower variance and a weaker climatic signal than that of the whole wood. Likewise, varying proportions of these wood compounds within the annual ring can smooth the isotopic signature after carbonisation, potentially explaining the observed differences in the LW profile of the NDP sample for the year 1143 after undergoing the carbonisation process (Fig. 6b and 7b). While this decrease in variance may impact the extraction of long-term climatic trends from charcoals, our data shows that information regarding extreme events is still preserved when large year-to-year isotopic shifts are present (Fig. 8). Additionally, focusing the analysis on either the EW or LW portions of each ring instead of the whole ring increases the robustness of the study, especially concerning oak trees, where early-seasonal growth largely relies on stored carbon (Helle and Schleser, 2004; Klein et al., 2016). Even with only one sample studied per period, the results from our laser ablation experiment are in line with these findings (Fig. 8). The EW $\delta^{13}C$ profiles in both experimental and NDP samples exhibit either an enrichment or a depletion in ^{13}C relative to the preceding latewood values, showing the influence of the previous year's reserves on current earlywood formation. Previous studies have yielded similar results but suggested that, in the presence of adverse growing conditions or prolonged climatic trends, oak trees can adapt their physiological strategies and alter these intra-seasonal dynamics (Kimak and Leuenberger, 2015; McCarroll et al., 2017). In the context of the NDP charred woods, drought stress events during the medieval climate anomaly are of particular interest, not only because the recurrence of droughts impacts soil water availability but also due to the potential influence of woodland management practices to reduce competition for water resources and ensure the quality of the timber. Current information on the physical characteristics of the longest beams incorporating the NDP roof structure— about a hundred years old, medium-diameter, straight, and knot-free long logs— suggests specific woodland management practices tailored for Gothic carpentry (Penagos et al., 2022). Depending on the site's dryness, the implementation of forestry practices can greatly modify the moisture and light conditions within the stand and thereby trigger distinct isotopic shifts in the remaining trees (Di Matteo et al., 2010).

In summary, the experimental assessment conducted here shows that regardless of the charring duration, at temperatures above 500 °C, inter- and intra-annual $\delta^{13}C$ signatures are preserved (Fig. 9). Although the $\delta^{13}C$ values of charred samples decrease towards those of the more resistant and slightly less variable lignin, several studies have shown that in general the correlations between $\delta^{13}C$ and climatic variables are preserved (Harlow et al., 2006; Loader et al., 2003). The further inclusion of $\delta^{13}C$ intra-annual variations in the study of the charred woods from NDP will allow a more detailed characterisation of a broad range of environmental changes and gain a more in-depth understanding of the different interaction(s) between climate–forest–woodland management systems during the High Middle Ages. To this end, the laser ablation system offers great potential, especially for charcoal samples with very narrow rings that might otherwise limit the development of a continuous and robust chronology.

Combined with wood anatomical features, $\delta^{13}C$ can provide an integrated approach to disentangle the complex physiological processes

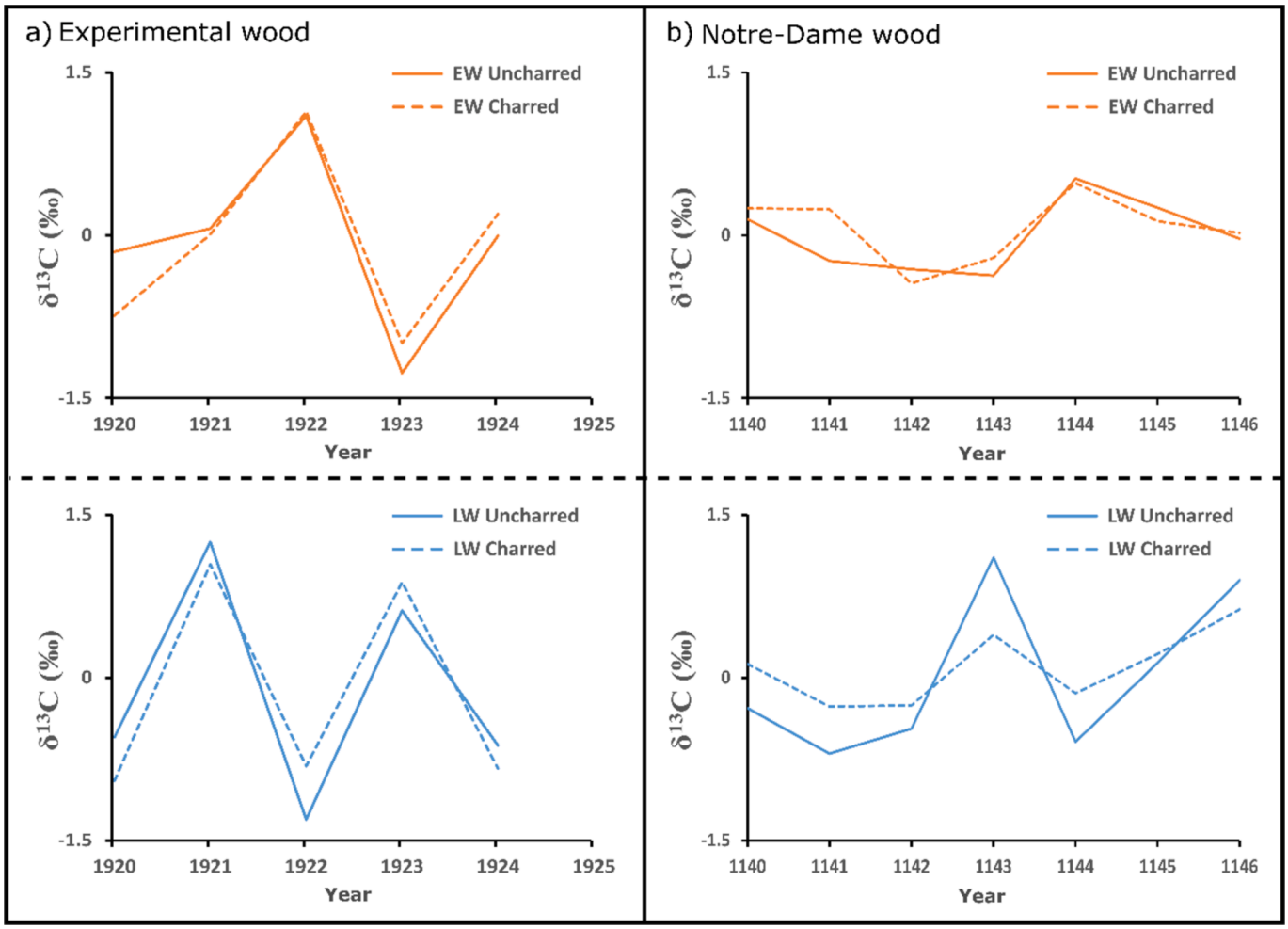

Fig. 7. Intra-annual $\delta^{13}C$ variability (first-differenced values) for (a) the experimental and (b) NDP samples developed using the laser ablation method (LA-IRMS).

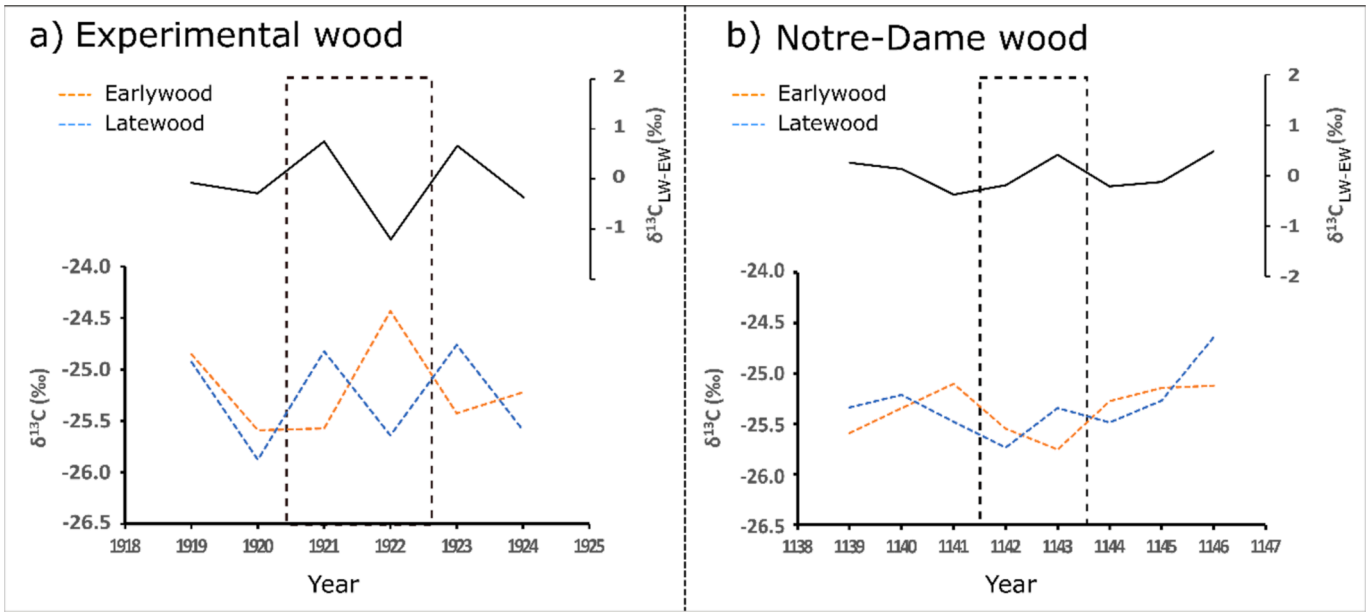

Fig. 8. Early and latewood $\delta^{13}C$ composition for the (a) experimental (1919–1924) and (b) NDP (1139–1146) charred samples. The top panel ($\delta^{13}C_{LW-EW}$) shows the difference between the $\delta^{13}C$ of LW and $\delta^{13}C$ of EW for each year.

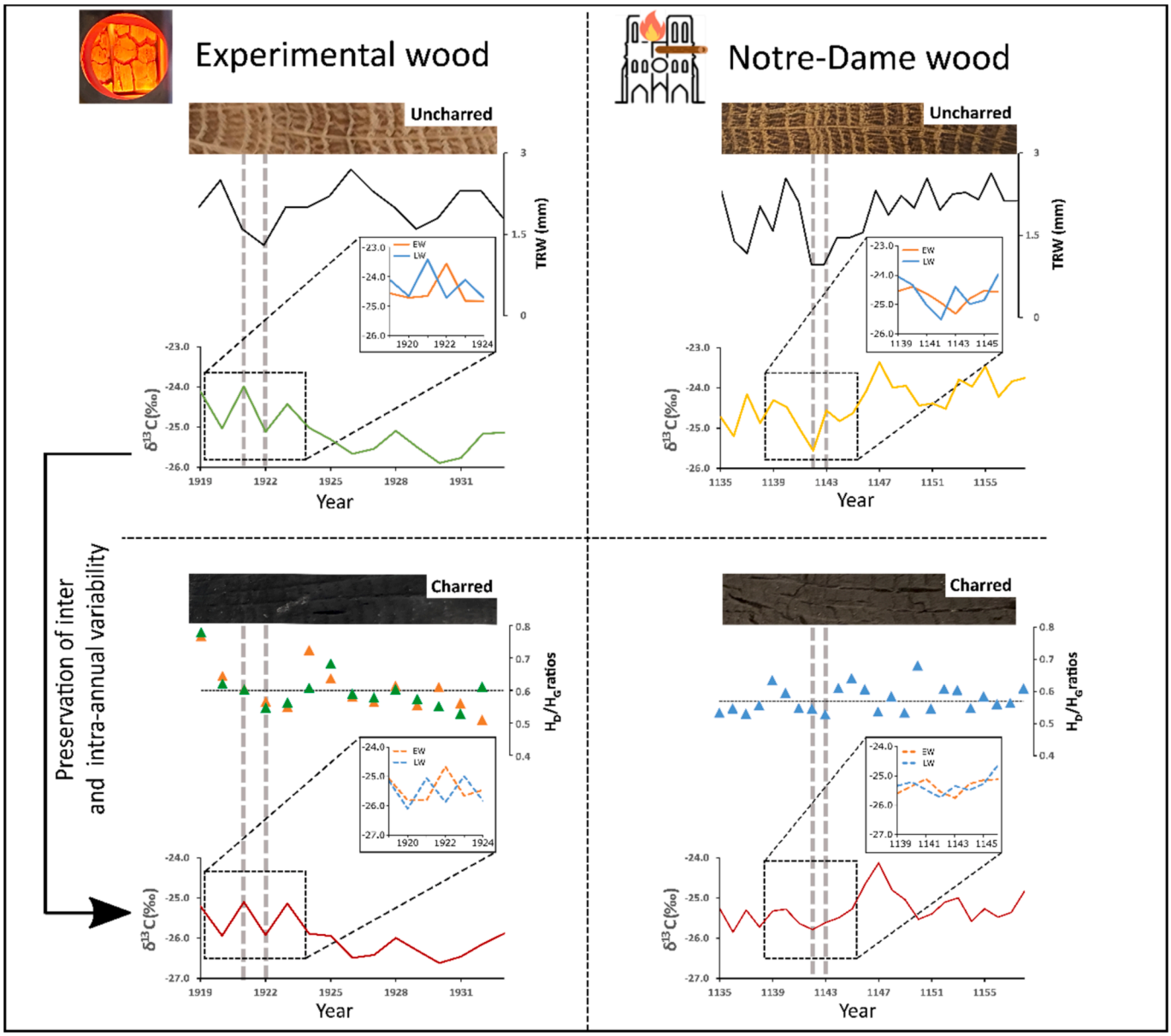

Fig 9. Schematic presentation of the different parameters incorporated in this study to investigate the preservation of the $\delta^{13}C$ inter and intra-annual variability after carbonisation.

that impacted the oak "Forest" of NDP.

CRediT authorship contribution statement

Eva Rocha: Writing – original draft, Investigation, Funding acquisition, Formal analysis, Data curation, Conceptualization. **Alexa Dufraisse:** Writing – review & editing, Supervision, Project administration, Methodology, Funding acquisition, Conceptualization. **Katja T. Rinne-Garmston:** Writing – review & editing, Investigation. **Elina Sahlstedt:** Writing – review & editing, Investigation. **Mercedes Mendez-Millan:** Writing – review & editing, Investigation. **Thanh Thuy Nguyen Tu:** Writing – review & editing. **Olivier Girardclos:** Investigation. **Michel Lemoine:** Methodology, Formal analysis. **Amir Ghavidel:** Writing – review & editing, Investigation. **Lucas Terrei:** Writing – review & editing, Methodology, Investigation, Formal analysis. **Anthony Collin:** Writing – review & editing, Methodology. **Ludovic Bellot-Gurlet:** Investigation. **Frédéric Delarue:** Writing – review & editing, Supervision, Project administration, Methodology, Investigation, Funding acquisition, Formal analysis, Conceptualization.

Declaration of competing interest

The authors declare that they have no known competing financial interests or personal relationships that could have appeared to influence the work reported in this paper.

Acknowledgements

We thank the ALYSES facility (IRD-SU) for access to the EA-IRMS instrument, supported by grants from Région Île-de-France. For the Raman measurements, we would like to thank Assia Hessani (MONARIS laboratory) for her technical assistance in carrying out the measurements on the "Plateforme de spectroscopies vibrationnelles et optiques (PLASVO, Sorbonne Université)". The study received financial support from the ANR (ANR CASIMODO – ANR-20-CE03-0008), Sorbonne Université, and the European Union's Horizon 2020 research and

innovation programme under the Marie Skłodowska-Curie grant agreement No (101111028). We thank the anonymous reviewers for their valuable comments and suggestions that helped improve the manuscript.

Data availability

Data will be made available on request.

References

Aguilera, M., Espinar, C., Ferrio, J.P., Pérez, G., Voltas, J., 2009. A map of autumn precipitation for the third millennium BP in the Eastern Iberian Peninsula from charcoal carbon isotopes. J. Geochem. Explor. 102 (3), 157–165. https://doi.org/10.1016/j.gexplo.2008.11.019.

Aguilera, M., Ferrio, J.P., Pérez, G., Araus, J.L., Voltas, J., 2012. Holocene changes in precipitation seasonality in the western Mediterranean Basin: A multi-species approach using δ13C of archaeobotanical remains. J. Quat. Sci. 27 (2), 192–202. https://doi.org/10.1002/jqs.1533.

Ascough, P.L., Bird, M.I., Wormald, P., Snape, C.E., Apperley, D., 2008. Influence of production variables and starting material on charcoal stable isotopic and molecular characteristics. Geochim. Cosmochim. Acta 72 (24), 6090–6102. https://doi.org/10.1016/j.gca.2008.10.009.

Audiard, B., Blasco, T., Brossier, B., Fiorentino, G., Battipaglia, G., Théry-Parisot, I., 2018. δ13C referential in three Pinus species for a first archaeological application to Paleolithic contexts: "Between intra- and inter-individual variation and carbonization effect". J. Archaeol. Sci. Rep. 20, 775–783. https://doi.org/10.1016/j.jasrep.2018.06.029.

Baton, F., Tu, T.T., Derenne, S., Delorme, A., Delarue, F., 2017. Tree-ring δ13C of archeological charcoals as indicator of past climatic seasonality. A case study from the Neolithic settlements of Lake Chalain (Jura, France). Quat. Int. 457, 50–59. https://doi.org/10.1016/j.quaint.2017.03.015.

Bird, M.I., Ascough, P.L., 2012. Isotopes in pyrogenic carbon: A review. Org Geochem. 42 (12), Article 12. https://doi.org/10.1016/j.orggeochem.2010.09.005.

Blondel, F., Cabanis, M., Girardclos, O., Grenouillet-Paradis, S., 2018. Impact of carbonization on growth rings: Dating by dendrochronology experiments on oak charcoals collected from archaeological sites. Quat. Int. 463, 268–281. https://doi.org/10.1016/j.quaint.2017.03.030.

Borella, S., Leuenberger, M., Saurer, M., Siegwolf, R., 1998. Reducing uncertainties in δ13C analysis of tree rings: Pooling, milling, and cellulose extraction. J. Geophys. Res. Atmos. 103 (D16), 19519–19526. https://doi.org/10.1029/98JD01169.

Braadbaart, F., Poole, I., 2008. Morphological, chemical and physical changes during charcoalification of wood and its relevance to archaeological contexts. J. Archaeol. Sci. 35 (9), 2434–2445. https://doi.org/10.1016/j.jas.2008.03.016.

Brossier, B., Poirier, P., 2018. A new method for facilitating tree-ring measurement on charcoal form archaeological and natural contexts. J. Archaeol. Sci. Rep. 19, 115–126. https://doi.org/10.1016/j.jasrep.2018.02.020.

Caracuta, V., Weinstein-Evron, M., Yeshurun, R., Kaufman, D., Tsatskin, A., Boaretto, E., 2016. Charred wood remains in the natufian sequence of el-Wad terrace (Israel): New insights into the climatic, environmental and cultural changes at the end of the Pleistocene. Quat. Sci. Rev. 131, 20–32. https://doi.org/10.1016/j.quascirev.2015.10.034.

Coplen, T.B., 1995. Discontinuance of SMOW and PDB. Nature 375 (6529). https://doi.org/10.1038/375285a0. Article 6529.

Czimczik, C.I., Preston, C.M., Schmidt, M.W.I., Werner, R.A., Schulze, E.-D., 2002. Effects of charring on mass, organic carbon, and stable carbon isotope composition of wood. Org Geochem. 33 (11), 1207–1223. https://doi.org/10.1016/S0146-6380(02)00137-7.

Deldicque, D., Rouzaud, J.-N., Velde, B., 2016. A Raman – HRTEM study of the carbonization of wood: A new Raman-based paleothermometer dedicated to archaeometry. Carbon 102, 319–329. https://doi.org/10.1016/j.carbon.2016.02.042.

Deldicque, D., Rouzaud, J.-N., 2020. Temperatures reached by the roof structure of Notre-Dame de Paris in the fire of April 15th 2019 determined by Raman paleothermometry. Comptes Rendus. Géoscience 352 (1), 7–18. https://doi.org/10.5802/crgeos.9.

Di Matteo, G., De Angelis, P., Brugnoli, E., Cherubini, P., Scarascia-Mugnozza, G., 2010. Tree-ring Δ13C reveals the impact of past forest management on water-use efficiency in a Mediterranean oak coppice in Tuscany (Italy). Ann. For. Sci. 67 (5), Article 5. https://doi.org/10.1051/forest/2010012.

Dufraisse, A., Coubray, S., Picornell-Gelabert, L., Alcolea, M., Girardclos, O., Delarue, F., Nguyen Tu, T.T., 2022. Taming Trees, Shaping Forests, and Managing Woodlands as Resources for Understanding Past Societies. Contributions and Current Limits of Dendro-Anthracology and Anthraco-Isotopy. Front. Ecol. Evol. 10. https://www.frontiersin.org/article/10.3389/fevo.2022.823968.

Edvardsson, J., Edwards, T.W.D., Linderson, H., Hammarlund, D., 2014. Exploring climate forcing of growth depression in subfossil South Swedish bog pines using stable isotopes. Dendrochronologia 32 (1), 55–61. https://doi.org/10.1016/j.dendro.2013.08.002.

Esper, J., Konter, O., Krusic, P.J., Saurer, M., Holzkämper, S., Büntgen, U., 2015. Long-term summer temperature variations in the Pyrenees from detrended stable carbon isotopes. Geochronometria 42 (1). https://doi.org/10.1515/geochr-2015-0006.

Esper, J., Holzkämper, S., Büntgen, U., Schöne, B., Keppler, F., Hartl, C., George, S.S., Riechelmann, D.F.C., Treydte, K., 2018. Site-specific climatic signals in stable isotope records from Swedish pine forests. Trees 32 (3), 855–869. https://doi.org/10.1007/s00468-018-1678-z.

Etien, N., Daux, V., Masson-Delmotte, V., Stievenard, M., Bernard, V., Durost, S., Guillemin, M. T., Mestre, O., & Pierre, M. (2008). A bi-proxy reconstruction of Fontainebleau (France) growing season temperature from A.D. 1596 to 2000. Climate of the Past, 4(2), 91–106. DOi: 10.5194/cp-4-91-2008.

Ferrio, J.P., Alonso, N., López, J.B., Araus, J.L., Voltas, J., 2006. Carbon isotope composition of fossil charcoal reveals aridity changes in the NW Mediterranean Basin. Glob. Chang. Biol. 12 (7), 1253–1266. https://doi.org/10.1111/j.1365-2486.2006.01170.x.

Fiorentino, G., Ferrio, J.P., Bogaard, A., Araus, J.L., Riehl, S., 2015. Stable isotopes in archaeobotanical research. Veg. Hist. Archaeobotany 24 (1), 215–227. https://doi.org/10.1007/s00334-014-0492-9.

Grissino-Mayer, H.D., 2001. Evaluating Crossdating Accuracy: A Manual and Tutorial for the Computer Program COFECHA. Tree-Ring Res. 57 (2), 205–221.

Hafner, P., McCarroll, D., Robertson, I., Loader, N.J., Gagen, M., Young, G.H., Bale, R.J., Sonninen, E., Levanič, T., 2014. A 520 year record of summer sunshine for the eastern European Alps based on stable carbon isotopes in larch tree rings. Clim. Dyn. 43 (3), 971–980. https://doi.org/10.1007/s00382-013-1864-z.

Hall, G., Woodborne, S., Scholes, M., 2008. Stable carbon isotope ratios from archaeological charcoal as palaeoenvironmental indicators. Chem. Geol. 247 (3), 384–400. https://doi.org/10.1016/j.chemgeo.2007.11.001.

Harlow, B.A., Marshall, J.D., Robinson, A.P., 2006. A multi-species comparison of δ13C from whole wood, extractive-free wood and holocellulose. Tree Physiol. 26 (6), 767–774. https://doi.org/10.1093/treephys/26.6.767.

Helama, S., Arppe, L., Timonen, M., Mielikäinen, K., Oinonen, M., 2018. A 7.5 ka chronology of stable carbon isotopes from tree rings with implications for their use in palaeo-cloud reconstruction. Global Planet. Change 170, 20–33. https://doi.org/10.1016/j.gloplacha.2018.08.002.

Helle, G., Schleser, G.H., 2004. Beyond CO2-fixation by Rubisco – an interpretation of 13C/12C variations in tree rings from novel intra-seasonal studies on broad-leaf trees. Plant Cell Environ. 27 (3), 367–380. https://doi.org/10.1111/j.0016-8025.2003.01159.x.

Hoffsummer, P. (2009). Roof Frames from the 11th to the 19th Century: Typology and development in Northern France and in Belgium: Analysis of CRMH Documentation. https://www.semanticscholar.org/paper/Roof-Frames-from-the-11th-to-the-19th-Century%3A-and-Hoffsummer/158699ca949a5f573b217abcd00dc9dc34d898ee.

Kimak, A., Leuenberger, M., 2015. Are carbohydrate storage strategies of trees traceable by early–latewood carbon isotope differences? Trees 29 (3), 859–870. https://doi.org/10.1007/s00468-015-1167-6.

Klein, T., Vitasse, Y., Hoch, G., 2016. Coordination between growth, phenology and carbon storage in three coexisting deciduous tree species in a temperate forest. Tree Physiol. 36 (7), 847–855. https://doi.org/10.1093/treephys/tpw030.

Labuhn, I., Daux, V., Girardclos, O., Stievenard, M., Pierre, M., Masson-Delmotte, V., 2016. French summer droughts since 1326 CE: A reconstruction based on tree ring cellulose $\delta^{18}O$. Clim. Past 12 (5), 1101–1117. https://doi.org/10.5194/cp-12-1101-2016.

Leavitt, S.W., Chase, T.N., Rajagopalan, B., Lee, E., Lawrence, P.J., Woodhouse, C.A., 2007. Southwestern U.S. drought maps from pinyon tree-ring carbon isotopes. Eos Trans. AGU 88 (4), 39–40. https://doi.org/10.1029/2007EO040005.

Li, G., Gao, L., Liu, F., Qiu, M., Dong, G., 2022. Quantitative studies on charcoalification: Physical and chemical changes of charring wood. Fundam. Res. https://doi.org/10.1016/j.fmre.2022.05.014.

Liu, X., Shao, X., Wang, L., Liang, E., Qin, D., Ren, J., 2008. Response and dendroclimatic implications of δ13C in tree rings to increasing drought on the northeastern Tibetan Plateau. J. Geophys. Res. Biogeosci. 113 (G3). https://doi.org/10.1029/2007JG000610.

Loader, N.J., Robertson, I., McCarroll, D., 2003. Comparison of stable carbon isotope ratios in the whole wood, cellulose and lignin of oak tree-rings. Palaeogeogr. Palaeoclimatol. Palaeoecol. 196 (3–4). https://doi.org/10.1016/S0031-0182(03)00466-8. Article 3–4.

Loader, N.J., Young, G.H.F., Grudd, H., McCarroll, D., 2013. Stable carbon isotopes from Torneträsk, northern Sweden provide a millennial length reconstruction of summer sunshine and its relationship to Arctic circulation. Quat. Sci. Rev. 62, 97–113. https://doi.org/10.1016/j.quascirev.2012.11.014.

Marshall, J.D., Brooks, J.R., Talhelm, A.F., 2022. Forest Management and Tree-Ring Isotopes. In: Siegwolf, R.T.W., Brooks, J.R., Roden, J., Saurer, M. (Eds.), Stable Isotopes in Tree Rings: Inferring Physiological, Climatic and Environmental Responses. Springer International Publishing, pp. 651–673. https://doi.org/10.1007/978-3-030-92698-4_23.

Masson-Delmotte, V., Raffalli-Delerce, G., Danis, P.A., Yiou, P., Stievenard, M., Guibal, F., Mestre, O., Bernard, V., Goosse, H., Hoffmann, G., Jouzel, J., 2005. Changes in European precipitation seasonality and in drought frequencies revealed by a four-century-long tree-ring isotopic record from Brittany, western France. Clim. Dyn. 24 (1), 57–69. https://doi.org/10.1007/s00382-004-0458-1.

McCarroll, D., Loader, N.J., 2004. Stable isotopes in tree rings. Quat. Sci. Rev. 23 (7), 771–801. https://doi.org/10.1016/j.quascirev.2003.06.017.

McCarroll, D., Whitney, M., Young, G.H.F., Loader, N.J., Gagen, M.H., 2017. A simple stable carbon isotope method for investigating changes in the use of recent versus old carbon in oak. Tree Physiol. 37 (8), 1021–1027. https://doi.org/10.1093/treephys/tpx030.

Mouraux, C., Delarue, F., Bardin, J., Nguyen Tu, T.T., Bellot-Gurlet, L., Paris, C., Coubray, S., Dufraisse, A., 2022. Assessing the carbonisation temperatures recorded

by ancient charcoals for δ13C-based palaeoclimate reconstruction. Sci. Rep. 12 (1), 14662. https://doi.org/10.1038/s41598-022-17836-2.

Paradis-Grenouillet, S., Dufraisse, A., 2018. Deciduous oak/chestnut: Differential shrinkage of wood during charcoalification? Preliminary experimental results and implications for wood diameter study in anthracology. Quat. Int. 463, 258–267. https://doi.org/10.1016/j.quaint.2017.06.074.

Penagos, C., Girardclos, O., Hunot, J.-Y., Martin, C., Jacquot, K., Cao, I., Lemoine, M., Brossier, B., Lavier, C., Coubray, S., Dufraisse, A., 2022. Naming, relocating and dating the woods of Notre-Dame "forest", first results based on collated data and archaeological surveys of the remains. J. Cult. Herit. https://doi.org/10.1016/j.culher.2022.09.004.

Rinne, K.T., Saurer, M., Kirdyanov, A.V., Loader, N.J., Bryukhanova, M.V., Werner, R.A., Siegwolf, R.T.W., 2015. The relationship between needle sugar carbon isotope ratios and tree rings of larch in Siberia. Tree Physiol. 35 (11), 1192–1205. https://doi.org/10.1093/treephys/tpv096.

Rouzaud, J.-N., Deldicque, D., Charon, É., Pageot, J., 2015. Carbons at the heart of questions on energy and environment: A nanostructural approach. C. R. Geosci. 347 (3), Article 3. https://doi.org/10.1016/j.crte.2015.04.004.

Scott, A.C., 2010. Charcoal recognition, taphonomy and uses in palaeoenvironmental analysis. Palaeogeogr. Palaeoclimatol. Palaeoecol. 291 (1–2), 11–39. https://doi.org/10.1016/j.palaeo.2009.12.012.

Siegwolf, R. T. W., Brooks, J. R., Roden, J., & Saurer, M. (Eds.). (2022). Stable Isotopes in Tree Rings: Inferring Physiological, Climatic and Environmental Responses (Vol. 8). Springer International Publishing. DOi: 10.1007/978-3-030-92698-4.

Štulc, A. I. (2023). Provenances géographiques des bois de la cathédrale de Notre-Dame de Paris. Compositions élémentaires et isotopiques en Sr et Nd: Effet de la carbonisation, référentiels régionaux et applications. [Unpublished doctoral dissertation]. Muséum national d'histoire naturelle.

Terrei, L., Acem, Z., Georges, V., Lardet, P., Boulet, P., Parent, G., 2019. Experimental tools applied to ignition study of spruce wood under cone calorimeter. Fire Saf. J. 108, 102845. https://doi.org/10.1016/j.firesaf.2019.102845.

Terrei, L., Acem, Z., Marchetti, V., Lardet, P., Boulet, P., Parent, G., 2021. In-depth wood temperature measurement using embedded thin wire thermocouples in cone calorimeter tests. Int. J. Therm. Sci. 162, 106686. https://doi.org/10.1016/j.ijthermalsci.2020.106686.

Turney, C.S.M., Wheeler, D., Chivas, A.R., 2006. Carbon isotope fractionation in wood during carbonization. Geochim. Cosmochim. Acta 70 (4), Article 4. https://doi.org/10.1016/j.gca.2005.10.031.

Young, G.H.F., Bale, R.J., Loader, N.J., Mccarroll, D., Nayling, N., Vousden, N., 2012. Central England temperature since AD 1850: The potential of stable carbon isotopes in British oak trees to reconstruct past summer temperatures. J. Quat. Sci. 27 (6), 606–614. https://doi.org/10.1002/jqs.2554.

Zhao, X.-Y., Qian, J.-L., Wang, J., He, Q.-Y., Wang, Z.-L., & Chen, C.-Z. (2006). Using a Tree Ring δ13C Annual Series to Reconstruct Atmospheric CO2 Concentration over the Past 300 Years1 1Project supported by the National Natural Science Foundation of China (No. 49771001). Pedosphere, 16(3), 371–379. DOi: 10.1016/S1002-0160(06)60065-9.